Inter-annual and seasonal variations in optical and physical characteristics of columnar aerosols over the Pokhara Valley in the Himalayan foothills

S. Ramachandran[a,b,*], Maheswar Rupakheti[b]

[a] Physical Research Laboratory, Ahmedabad, India
[b] Institute for Advanced Sustainability Studies, Potsdam, Germany

ABSTRACT

This study reports comprehensive analysis of seasonal and inter-annual variations of aerosol optical and physical properties over the Pokhara Valley in the foothills of central Himalayas in Nepal utilizing the high-quality multi-year columnar aerosol data observed recently from January 2010 to December 2017. The influence of forest fires and agro-residue fires on aerosol properties is also investigated. Seasonal mean aerosol optical depth (AOD) over Pokhara is ≥ 0.3 during the year, highest in pre-monsoon and lowest in monsoon season. AOD exhibits a consistent seasonal cycle every year with a peak in pre-monsoon. Fine mode fraction contributing to AOD and Ångström exponent (α) corroborate seasonal pattern of AODs. AODs show good correlation with fire counts in the Pokhara Valley and surrounding region. The aerosol volume size distributions are bimodal. The peaks in volume size distribution and volume concentrations obtained in 2016 pre-monsoon are the highest during the 8-year observation period which coincided with peaks in the occurrence of highest number of fires in the Pokhara Valley and surrounding region. Effective radius of coarse mode aerosols is an order of magnitude larger than fine mode aerosols. The analysis of optical and physical properties of aerosols over the Pokhara Valley suggest that the aerosols observed over the Himalayan foothills are of urban/industrial, biomass burning and dust origin with proportional contributions varying in different seasons. The study provides observational constraints on aerosol physical and optical properties that can serve as inputs for model simulation of aerosol physiochemical processes and quantification of impacts on air quality, climate and sensitive ecosystems in this data-sparse region.

1. Introduction

The Himalayas and the surrounding regions are characterized with several sensitive ecosystems of global importance, as well as highly vulnerable populations, yet, they remain one of the least studied regions in the world. The Himalayan foothill region, situated between heavily-polluted Indo-Gangetic Plains (IGP) to the south and the relatively cleaner Himalayan-Tibetan mountain regions to the north, provides a unique natural setting to study properties of aerosols originated within the foothills of the Himalayas and upwind regions such as IGP that are transported northwards to mountain regions, a poorly sampled region in terms of atmospheric observations. Air pollution is a major cause that impacts the Himalayas and the surrounding regions, as not only the health of large populace of people and ecosystems are affected, but also the crops, climate, cryosphere and monsoon patterns (Saikawa et al., 2019 and references therein). The air pollutants emitted from both natural and manmade sources such as biomass burning (e.g., burning fire wood, forest fires) and fossil fuel combustions within and

upwind of the region constitute the aerosols present over the Himalayas and the Tibetan Plateau region. Aerosols exhibit large temporal and spatial variations across the Himalayas (Lüthi et al., 2015; Rupakheti et al., 2019; Singh et al., 2019; Chen et al., 2019). Atmospheric dynamics plays an important role in the transport, transformation and removal of aerosols from west Asia, the Indo-Gangetic Plains (IGP) to the Himalayan foothills and the Tibetan Plateau regions (Lüthi et al., 2015; Singh et al., 2019 and references therein). The effects of boundary layer dynamics on $PM_{2.5}$ and black carbon (BC) aerosol mass concentrations have been studied over the IGP, at the foothills of the Himalayas, and the Himalayan mountain region (Raatikainen et al., 2014; Putero et al., 2018). Earlier studies showed that the aerosol loading peaks in the region generally during pre-monsoon season (Gautam et al., 2011; Raatikainen et al., 2014; Singh et al., 2019; Rupakheti et al., 2019). Diverse aerosol emissions (dust, BC, nitrate, sulfate and organics) from natural and manmade sources give rise to a persistent blanket of haze characterized by heavy aerosol loading over the IGP and downwind regions, including the Himalayan foothills,

almost throughout the year (Ramanathan et al., 2007a; Lawrence and Lelieveld, 2010; Kedia et al., 2014; Cho et al., 2017). The quantification of aerosol properties over heavily polluted source regions in South Asia, notably the IGP, as well as the downwind regions that receive the pollution outflow, such as the Himalayan mountains, are still highly uncertain as these regions are still poorly sampled (Gustafsson and Ramanathan, 2016; Lawrence and Lelieveld, 2010). Further, model simulation of aerosol characteristics in high-altitude locations, including the Himalayan-Tibetan Plateau region, is uncertain due to complex orography and transport occurring on vertical and horizontal scales including convection and local mountain-valley circulations in the complex topography (IPCC, 2013; Myhre et al., 2013).

The Himalayan foothill region is affected every year by biomass burning emissions within the region and from north India (Lüthi et al., 2015; Rupakheti et al., 2017; Bhardwaj et al., 2018; Mahata et al., 2018; Singh et al., 2019). These biomass burning emissions occur during pre-monsoon and post-monsoon seasons due to forest fires, and burning of crop waste. In addition, the emissions from fuels used in domestic cooking and heating constitute biomass burning which is active throughout the year over this region. Earlier studies showed enhancement in ozone (O_3) and carbon monoxide (CO) levels during these seasons due to the biomass burning emissions in the IGP and Himalayan foothills in India and Nepal (Rupakheti et al., 2017; Bhardwaj et al., 2018; Mahata et al., 2018). Recently the impacts of intense haze events on aerosol optical properties and radiative forcing over Lumbini in southern Nepal were reported, which is a result of regional urban/industrial and biomass burning emissions transported to Lumbini region under favorable meteorological conditions (Rupakheti et al., 2020). On local and global scales, identifying the factors that drive climate change, including air pollution, are crucial to effectively reduce emissions and their impacts (Meng et al., 2019). The global emissions of fine PM and its precursor gases continued to grow between 2004 and 2011 (Meng et al., 2019). Emissions of key air pollutants and climate forcing species (e.g., BC, SO_2, CO) in South Asia showed slightly increasing trends during 2004–2011 (Meng et al., 2019). In the previous studies, physical, chemical and optical properties of aerosols obtained over the Himalayas (including a couple of sites in the Himalayan foothills such as Pokhara, Hetauda, Kathmandu in Nepal) have been analyzed (e.g., Gautam et al., 2011; Raatikainen et al., 2014; Cho et al., 2017), however, almost all the studies have been limited either to a particular season or a one/two years of data, a limited set of aerosol properties, and/or only surface or only columnar measurements. Model simulations of aerosol characteristics in high-altitude locations over a mountainous region are difficult, and uncertain as mentioned earlier. Remote

sensing (satellite) of aerosols can provide regional/global coverage, however, they lack in accuracy and resolution. For example, the uncertainty/error estimate in MODIS AODs is a function of AOD value ($\pm 0.05 \pm 0.15$AOD) (Levy et al., 2013). The satellite AODs also were found to not compare well with AODs observed with the in situ Aerosol Robotic Network (AERONET) in mountainous regions (Levy et al., 2013). Further, remote sensing observations have limitations as they can retrieve only a few aerosol characteristics, such as columnar content (AOD), as compared to ground-based measurements (e.g., it is difficult to retrieve aerosol size distribution). Vertical profiles of aerosol extinction from space-based lidar are available from CALIPSO at a horizontal resolution of 40 km, and the measurement uncertainty is about 40% (http://wdc.clr.de/sensors/calipso). Further, the sampling frequency is lower, as CALIPSO repeats orbit once in 16 days over the same location, and therefore an exact overpass over a particular or the same location occurs only once (or at the most twice) in a month. Thus, ground-based in situ measurements available almost on a daily basis are more accurate, and best suited to examine the seasonal and inter-annual variabilities of aerosol characteristics over Pokhara Valley, a high-altitude location situated in a mountain region.

In this study, for the first time, we comprehensively analyze the seasonal and inter-annual variations of all the relevant key columnar aerosol properties, relevant in the context of climate change, observed over the Pokhara Valley in Nepal, a site in the Himalayan foothills using the high-quality data obtained from January 2010 to December 2017. The seasonal as well as year-to-year variations in aerosol levels, properties and their radiative effects over the Himalayan foothill region (true for other regions as well) is expected to be influenced by the seasonal emission strengths of different sources and source regions and the seasonal meteorology during the year, and the inter-annual levels are mainly controlled by the changes in emission strengths rather than the inter-annual meteorological variations, as reported in a previous study which found that the effects of inter-annual meteorological variations on $PM_{2.5}$ concentrations during 2013–17 were relatively small in eastern China (Zhang et al., 2019). In addition, we investigate and quantify the influence of fires (forest fires and agro-residue burning fires) in the region on aerosol properties observed over Pokhara. In a first of its kind examination, we determine the extent of influence/contribution of local and regional scale biomass burning emissions (fires mentioned above) on the physical and optical characteristics of aerosols over Pokhara during the 8-year period and their seasonal, and year to year variability. Furthermore, a regional scale analysis of optical and physical characteristics of aerosols from different locations across the IGP and the Himalayas (Figs. 1, 2) is also carried out with an
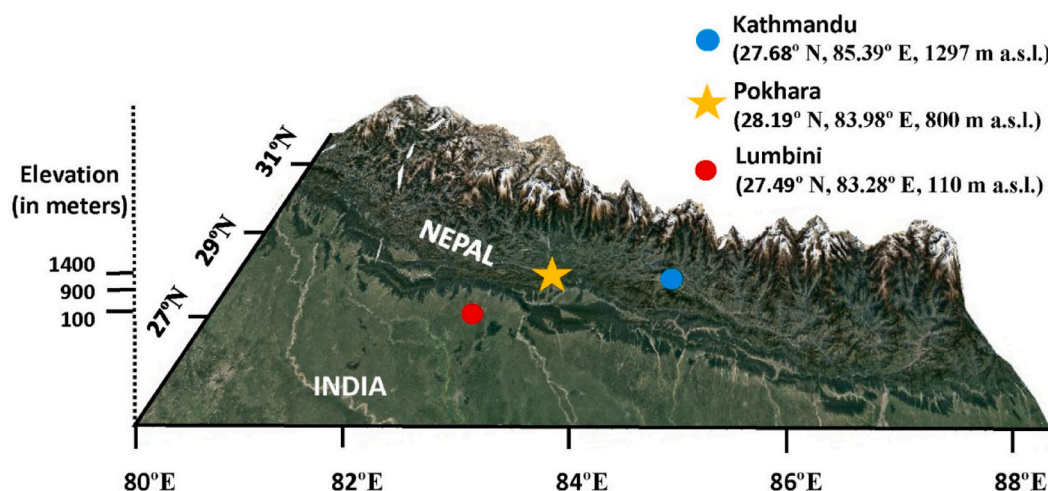

Fig. 1. Location of the AERONET Pokhara site in Nepal. AERONET Lumbini site in the northern edge of the Indo-Gangetic Plain (IGP) and Kathmandu site in the Himalayan foothills are also shown.
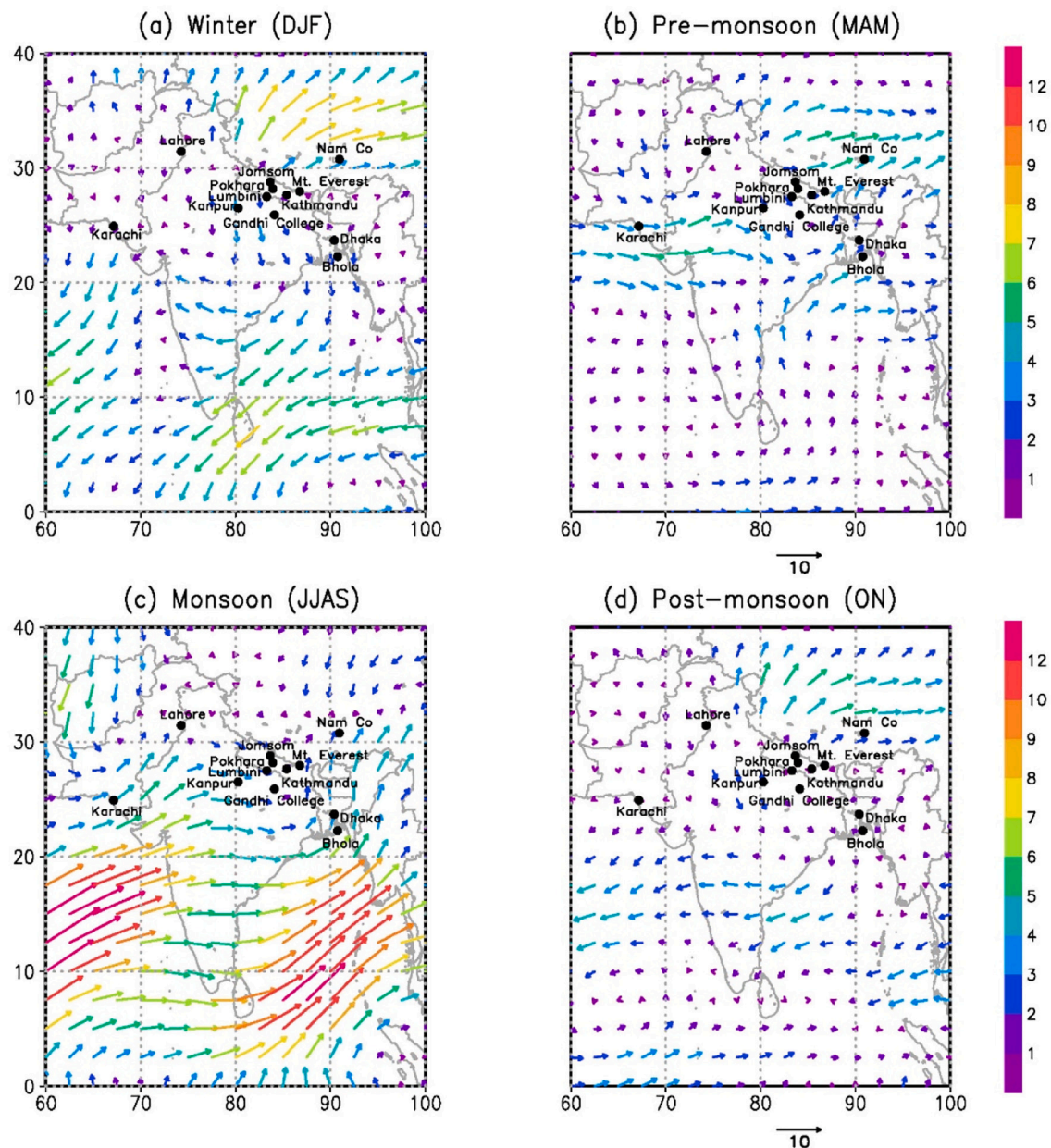
Fig. 2. Seasonal mean synoptic winds (in ms^{-1}) at 925 hPa over the Indo-Gangetic Plain and Nepal during (a) winter (DJF), (b) pre-monsoon (MAM), (c) monsoon (JJAS) and (d) post-monsoon (ON) for 2014–15. Wind data are downloaded from http://www.esrl.noaa.gov/psd/. The color scale represents the wind speed, and the length of the arrow given under (b) and (d) correpends to 10 ms^{-1}. Study locations in the Indo-Gangetic Plains, the Himalayan foothills and the Himalayas are shown in the plots.

objective to compare and contrast the aerosols observed in different seasons. The year to year variations in aerosol properties over the Himalayan foothills, a transition region between the highly polluted IGP, a global air pollution hotspot and the relatively cleaner Himalayan-Tibetan mountain regions, including the effect of fires on aerosols in the region, will be useful inputs for global/regional climate/chemistry circulation models and can help quantify and address the impacts of air pollution and climate change on such inter-disciplinary issues as agriculture, cryosphere, public health, and sustainable development of the greater Himalayan region.

2. Data and analysis

2.1. Measurement site and meteorological conditions

Pokhara Valley (28.2°N, 83.9°E, 800 m above mean sea level), located in the foothills of the central Himalayas, is the second largest metropolitan region in Nepal (Fig. 1). Pokhara Valley region experiences humid subtropical climate (hot, humid summer and cold, dry winter), and is influenced by the South Asian monsoon system (Singh et al., 2019). This region receives the highest amount of annual rainfall in Nepal. Based on the prevailing meteorological conditions the seasons over South Asia are classified as the winter (DJF: December, January, February), pre-monsoon (MAM: March, April, May), monsoon (JJAS: June, July, August, September) and post-monsoon (ON: October, November). The winter winds over Nepal, and generally over South Asia
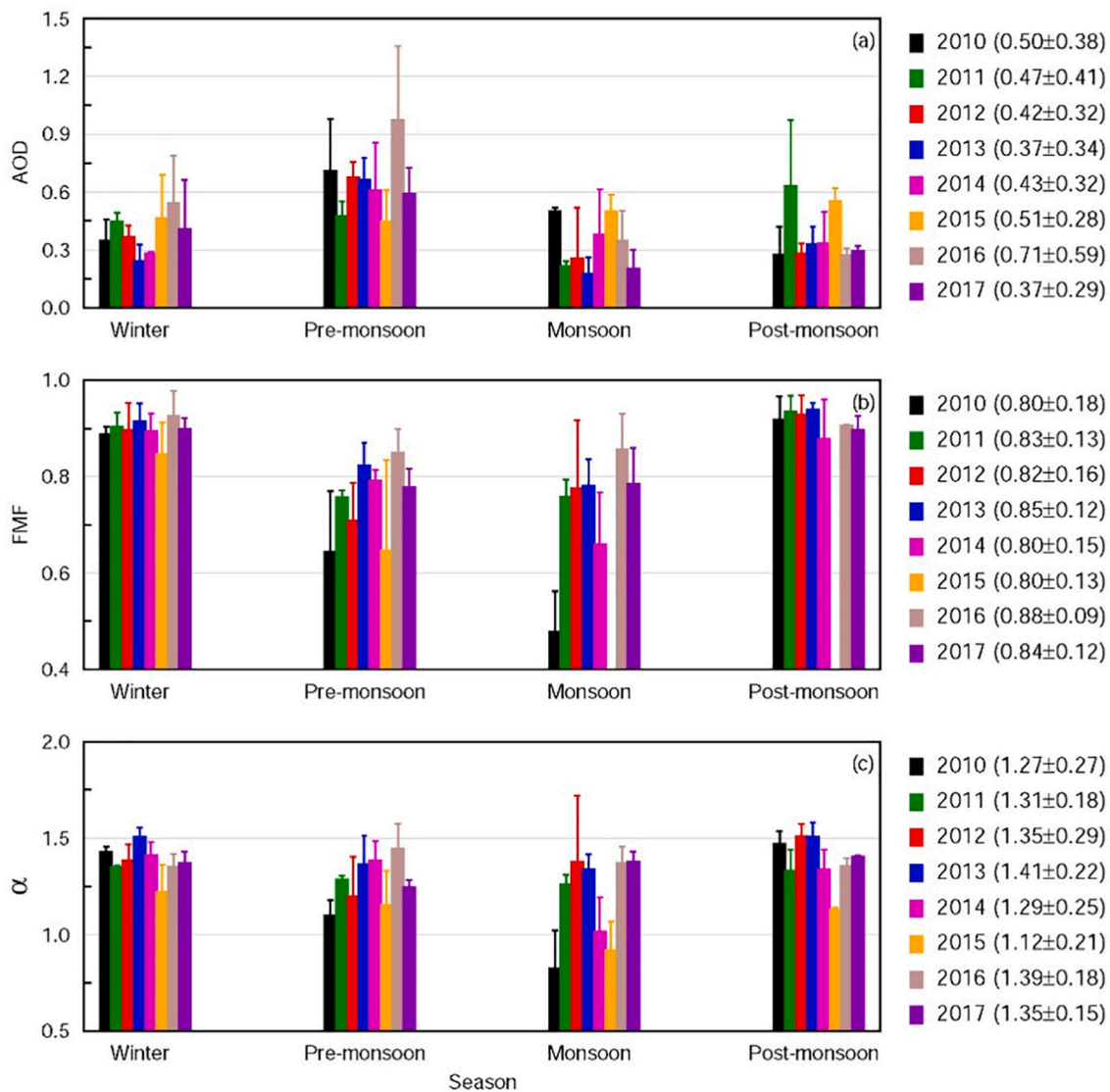
Fig. 3. Seasonal mean (a) aerosol optical depth (AOD) at 0.55 μm, (b) fine mode fraction (FMF) in AOD and (c) Ångström exponent (α) computed from the AODs in the 0.44–0.87 μm wavelength region for the years 2010 to 2017. The annual mean values of theseaerosol parameters and their ± 1σ (standard deviation) from the mean are given for each year.

(Fig. 2a) are calm, and northerly/northeasterly, which are conducive to accumulation of local and regional emissions and formation of annually recurrent regional scale atmospheric haze, referred to as atmospheric brown clouds (Ramanathan et al., 2007a). The pre-monsoon, and monsoon (or rainy season) winds, which are stronger than winter winds, are from southwesterly direction, and thus they transport dust from arid regions (pre-monsoon), and moist air masses laden with sea salt from the marine region and dust from arid regions to the west (monsoon) (Fig. 2b, c). The post-monsoon winds are calm and undergo transition in direction shifting from southwest to northeast (Fig. 2d).

2.2. AERONET measurements

The columnar aerosol content and aerosol size measured with ground-based CIMEL Sun/sky radiometers during 2010–2017 at the AERONET (Holben et al., 2001) (https://aeronet.gsfc.nasa.gov/) site at the Pokhara Valley are analyzed. The CIMEL Sun/sky radiometers measure direct solar and diffuse sky radiances in the spectral range of 0.34–1.02 μm (Holben et al., 2001). The field of view of the instrument is about 1.2° and it makes direct solar radiation measurements roughly every 15 min under clear sky condition. For direct solar measurement,

triplet observations are made at each wavelength for calibration (using Langley technique) and to screen the clouds. In the present study, direct solar measurements made at four spectral channels (0.44, 0.50, 0.675 and 0.87 μm), sky radiance measurements made at four spectral channels (0.44, 0.675, 0.87 and 1.02 μm), are utilized. Details on the measurement protocol for AERONET, calibration techniques, methodology, data processing and quality can be found in literature (Holben et al., 2001; Dubovik et al., 2000; O'Neill et al., 2003). The fine mode fraction (FMF) is calculated as the ratio of fine mode AOD (due to particles in 0.01–1.0 μm radius range) to total AOD (due to all particles in 0.01–10 μm radius range) at 0.50 μm from sky radiance measurements. The Ångström exponent (α) is determined from spectral AODs measured in the 0.44–0.87 μm wavelength range. The uncertainty in AODs estimated using the direct solar radiation measurements is < ± 0.01 for wavelengths > 0.44 μm and is < ± 0.02 for shorter wavelengths (Holben et al., 2001). The error in AERONET derived FMF is ~10% (O'Neill et al., 2003). The errors in the retrieved volume size distributions are not significant in the radius range of 0.1–7 μm (Dubovik et al., 2002).

At the AERONET sites observations are made at ca. 15–20 min time intervals under the clear-sky conditions, resulting in with typically
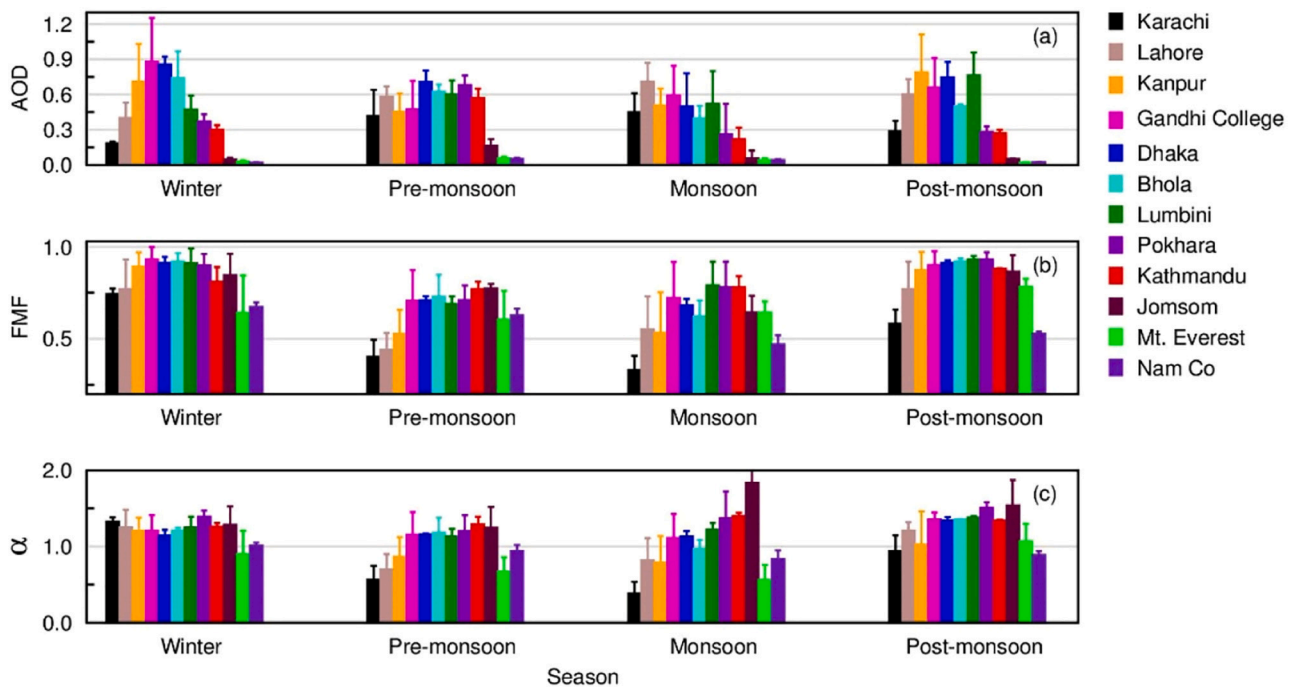
Fig. 4. Seasonal mean optical and physical properties of aerosols: (a) AOD, (b) FMF and (c) α obtained over Pokhara in comparison with other locations across the Indo-Gangetic Plain (IGP), the Himalayan foothills and the Himalayas (Fig. 1).

about 20 measurements every day. During the monsoon season though relatively less data is available, however, the retrieved aerosol properties are reliable as the observations during monsoon season also undergo the same level of quality control and cloud screening similar to the other seasons. The AERONET retrieved aerosol properties have the highest accuracy for observations when solar zenith angle is between 50° and 80° (García et al., 2008), and only those data that are within this solar zenith angle range are utilized in the study. In the present study, daily measurements collected during January 2010–December 2017 are used to calculate the monthly, seasonal and annual averages. As mentioned earlier since level 2, quality-controlled, cloud-screened and calibrated AERONET data are used in the study, the uncertainties in the aerosol parameters are not expected to change any conclusions of the study.

2.3. Fire counts

To study the influence of fires on aerosol properties, the data from MODIS sensors onboard the Terra and Aqua satellite platforms that detect fire spots globally on a daily basis at a spatial resolution of 1 km × 1 km are utilized. Detailed description of the MODIS fire detection algorithm is provided in Giglio et al. (2016), and further details are provided in the Algorithm Theoretical Document Basis (ATBD) (http://modis-fire.umd.edu/files/atbd_mod14.pdf). In the present study, we have utilized the MODIS Thermal Anomalies/Fire 5-Min L2 Swath 1-km data (Collection 006) retrieved from both Terra (MOD14) and Aqua (MYD14) platforms from the NASA Fire Information for Resource Management System (FIRMS) (https://firms.modaps.eosdis.nasa.gov/). In brief, each fire pixel detected by the thermal anomalies algorithm at 1-km resolution is categorized in three confidence classes based on its calculated confidence value (C) as *low*: 0% ≤ C < 30%, *nominal*: 30% ≤ C < 80%, and *high*: 80% ≤ C < 100%. The confidence level in the detection of fire spot indicates the quality of individual fire pixels. Fire pixel data with confidence value C > 30% assigned the confidence class of *nominal* and *high* are used in the present study, since both confidence classes ensure fewer false detection of fire pixels.

3. Results and discussion

3.1. Aerosol optical depth, fine mode fraction and Ångström exponent

The seasonal mean AOD (at 0.55 μm) is ≥ 0.3 over Pokhara during the 8-year period, except during 2011, 2012, 2013, and 2017 monsoon seasons (Fig. 3). Every year AOD follows a recurrent seasonal cycle over Pokhara – a gradual increase from January to April (peak) (winter to pre-monsoon), followed by a decrease leading to lowest values during monsoon months, and again a gradual increase through post-monsoon and winter until it peaks around April in pre-monsoon season. AODs > 0.3 over Pokhara (a high altitude site located at ca. 800 m asl) during most of post-monsoon, winter and pre-monsoon months indicate that the Pokhara Valley and surrounding region is heavily polluted (Ramanathan et al., 2007b) almost throughout the year. The extent of the influence of regional transport of emission on top of major local sources (e.g., Singh et al., 2019) will be discussed in the following section. The high aerosol content during winter and pre-monsoon over the Pokhara Valley (Singh et al., 2019) can be attributed to the strong convective activity in the IGP due to which polluted air masses near the surface get lifted to higher altitudes and get advected northwards to the Himalayan foothills and mountain regions (Kuhlmann and Quaas, 2010; Lüthi et al., 2015; Singh et al., 2019). The advection of air masses during pre-monsoon is also assisted by the strong updraft and the expansion of the planetary boundary layer (reported to be the highest in the pre-monsoon in the IGP); these air masses routinely mix with synoptic scale westerlies (Raatikainen et al., 2014; Putero et al., 2018; Singh et al., 2019), and give rise to the highest AOD during the pre-monsoon months (Fig. 3) every year. The FMF and α follow almost a similar pattern. FMF is > 0.80 during post-monsoon and winter, and decreases during pre-monsoon and monsoon. Furthermore, α is > 1 almost throughout the year, except it is < 1 in two monsoon season (2010 and 2015). Higher FMF and α during post-monsoon and winter confirm the dominant contribution of fine mode particles to AOD over the Pokhara Valley region. The lower FMF and α during pre-monsoon and monsoon suggest the presence of coarse particles (e.g., sea salt, dust) in the columnar aerosol distribution. The higher AOD, FMF and α
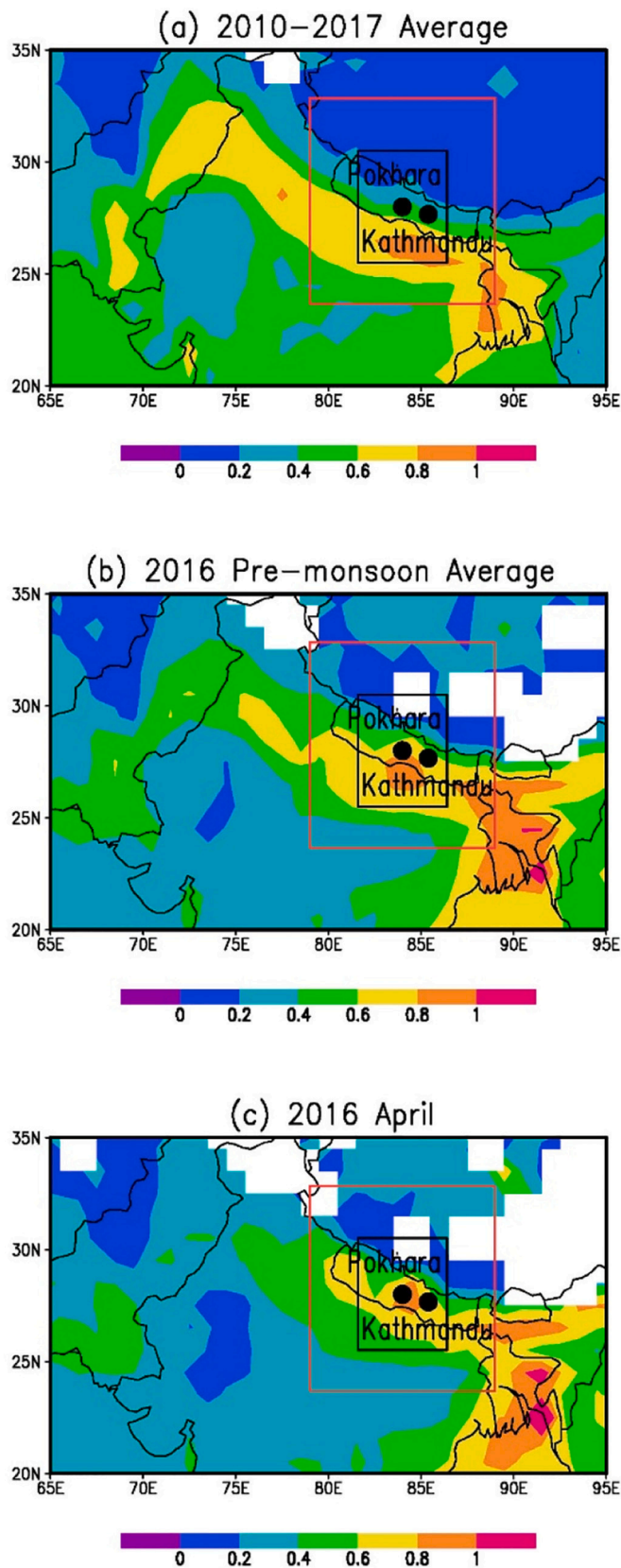
Fig. 5. The AOD (at 0.55 μm from MODIS) (a) averaged for 2010–2017 over the study region, (b) 2016 pre-monsoon (average of 2016 March–April-May), and (c) 2016 April. AOD data (MODIS Terra v6.1 Combined Dark Target and Deep Blue Algorithm) are downloaded from https://giovanni.gsfc.nasa.gov/giovanni/. The black and red boxes represent 5° latitude x 5° longitude, and 10° latitude x 10° longitude regions with Pokhara at the center respectively. White areas in the figure denote missing/unavailable data.

over Pokhara can be ascribed to accumulation and regional scale transport of the fine mode aerosols emitted by the anthropogenic activities (fossil fuel and biomass burning) over South Asia (especially the IGP, a heavily polluted region in South Asia, Fig. 2) into the atmosphere with calm winds during post-monsoon and winter. The lower AOD, FMF and α during pre-monsoon and monsoon occur due to southwesterly winds bringing in higher amount of dust from arid regions in South Asia and beyond as well as local soil dust from dry agricultural fields (Singh et al., 2019), and increase in wet deposition during monsoon and change in the origin of air parcels (Fig. 2b, c). Further, during the monsoon the AODs are governed by local emissions, since precipitation suppresses the transport of regional emissions; furthermore, some major seasonal sources like forest fires and brick production are not active during the monsoon season. The features in AOD, FMF and α obtained over Pokhara repeat year after year, however, with small differences in magnitude (Fig. 3).

A previous study (Gautam et al., 2011) reported AODs measured during a pre-monsoon campaign over a few locations in the Himalayan foothills during 2009 – at Hetauda (27.4°N, 85.0°E, 465 m asl) during 18 Apr-30 May 2009, and Dhulikhel 27.6°N, 85.5°E, 1500 m asl) during 11 Apr-16 Jun 2009 in Nepal. The AODs at Hetauda and Dhulikhel were comparable; 0.75 ± 0.50 and 0.73 ± 0.49 respectively. The AODs during pre-monsoon did not exhibit significant difference as the elevation increased from Hetauda to Dhulikhel. The respective α values were found to be 1.10 ± 0.27 and 1.23 ± 0.36. In comparison, seasonal mean AODs over Pokhara during pre-monsoon and monsoon seasons of 2010–2017 varied in the 0.20 to 1.0 range (Fig. 3a), while the α values are mostly between 1.0 and 1.5 (Fig. 3c). An exact one-on-one comparison is difficult between the current study and Gautam et al.'s study, as the location, time (days in the season) and the year are different between the two studies. The features seen in aerosol characteristics over Pokhara are contrastingly different to those obtained over Kanpur (ca. 400 km aerial distance away in the southwest direction from Pokhara), an urban location influenced by dust and anthropogenic emissions in the central IGP. For example, AODs over Kanpur decrease from January to March, increase from March to June, fall from June to September and then increase from October to December (Eck et al., 2010; Kedia et al., 2014). However, the monthly variation in α including its magnitude over Pokhara resembles that of Kanpur (Eck et al., 2010; Kedia et al., 2014). The monthly average α values were > 1.2 during winter and post-monsoon, and in the 0.4–1.0 range during pre-monsoon and monsoon months over Kanpur (Eck et al., 2010; Kedia et al., 2014). The higher values of α over Kanpur were attributed to the dominance of fine mode aerosols from combustion sources (e.g., coal fired power plants), industrial and vehicular emissions and domestic biomass burning (fuel wood and dung cake) (Eck et al., 2010); α values were lower due to the presence of coarse mode dust aerosols transported from arid regions to Kanpur (Eck et al., 2010; Kedia et al., 2014). Over Lumbini, located in the northern edge of the central IGP, the mean AOD during January 2013–December 2014 was found to be 0.64 ± 0.38 (Rupakheti et al., 2018) comparable to the AODs observed over Pokhara (Fig. 3a). More than 80% of the daily mean AODs over Lumbini were > 0.3 indicating polluted conditions in this semi-urban region as the levels of observed aerosol loading were comparable to the heavily polluted sites in the IGP (Rupakheti et al., 2018). Pokhara also has AODs similar to Lumbini. The monthly mean α values over Lumbini were in the 1.0–1.5 range (Rupakheti et al., 2018), similar to the α values observed over Pokhara (Fig. 3c).

AOD, FMF and α exhibit seasonal and regional scale variations across the IGP and the Himalayas (Fig. 4). Daily mean AOD, FMF and α obtained for 2013–2014/2015 over Karachi (24.95°N, 67.14°E, 49 m asl), Lahore (31.38°N, 74.26°E, 209 m asl), (Kanpur (26.51°N, 80.23°E, 123 m asl), Gandhi College (25.87°N, 84.13°E, 60 m asl), Dhaka (23.73°N, 90.39°E, 34 m asl), Bhola (22.23°N, 90.76°E, 7 m asl) all across the IGP, and Lumbini (27.49°N, 83.28°E, 110 m asl), Kathmandu (27.68°N, 85.39°E, 1297 m asl), Jomsom (28.78°N, 83.71°E, 2825 m

Table 1

Monthly fire counts from 2010 to 2017 over the Pokhara Valley, 5° latitude x 5° longitude grid centered around Pokhara, and 10° latitude x 10° longitude grid with Pokhara at the center (the black and red boxed areas respectively in Fig. 5). Fire pixel data with confidence value C > 30% assigned the confidence class of *nominal* and *high* which ensure fewer false detection of fire pixels used in the present study are given.

Year	Jan	Feb	Mar	Apr	May	Jun	Jul	Aug	Sep	Oct	Nov	Dec
Pokhara Valley												
2010	40	8	1	17								38
2011	14	23	7	8							1	32
2012	4	7	1	4	2						7	37
2013	40	1	1	27							1	17
2014	25	14	5	11	6							11
2015	4			1		2					2	18
2016	7	29	29	67	2					2	6	21
2017	17	12	9	4							6	57
5°x5° latitude-longitude region centered around Pokhara (black box in Fig. 5)												
2010	134	134	578	2005	132	27	3	2		4	78	168
2011	103	158	302	1061	234	9	1	1	1	20	199	194
2012	95	131	447	1911	800	112	4	2	1	19	298	174
2013	151	79	374	1591	236	2	4	1	12	12	129	143
2014	80	103	333	1758	606	35			1	1	153	115
2015	42	81	89	226	111	117	2		2	21	232	261
2016	194	329	1213	4401	184	2		1	2	17	260	161
2017	115	197	180	1667	227	9			7	25	306	194
10°x10° latitude-longitude region centered around Pokhara (red box in Fig. 5)												
2010	442	560	3859	5065	508	125	91	91	89	344	370	769
2011	468	735	2915	2488	914	78	73	56	68	293	542	611
2012	396	776	2127	3815	3049	519	24	47	67	336	773	860
2013	548	410	998	3042	1273	81	53	50	99	221	729	783
2014	393	477	963	3457	1676	461	43	47	90	351	754	578
2015	276	563	782	1227	959	451	38	41	102	529	793	1218
2016	760	952	2746	9474	833	86	19	57	58	662	1048	762
2017	447	775	1678	5105	900	144	30	62	117	561	1089	1057

asl), and Ev-K²-CNR (27.95°N, 86.82°E, 5079 m asl) near the base-camp of Mt. Everest (Nepal) (hereinafter referred to as Mt. Everest) located to the north and downwind of IGP in the Himalayas, and Nam Co (30.77°N, 90.96°E, 4746 m asl) on the Tibetan Plateau (China) are analyzed to examine the regional-scale variability, and to provide a regional snapshot of aerosol properties for a year. As the objective was to cover one annual cycle over all the study locations, data sets corresponding to years 2013–14, or 2014–15 were utilized. The years 2013–15 were chosen as the coincident data was available for almost all the months at most locations in this timeframe (2010–17). As for most of the other locations maximum amount of data was available for the year 2014, data for Pokhara was chosen for the year 2014 (Fig. 4) for comparison. However, as the aerosol optical properties measured over Pokhara exhibit consistent annual cycle during the 8-year period (2010–17) (Fig. 3) the inferences drawn based on the comparison (for year 2014) are not expected to change any conclusions significantly. The IGP (Figs. 1, 2), covers parts of Pakistan, India, Bangladesh and Nepal. During winter AOD increases from west to east (Karachi to Gandhi College) and decreases gradually from Gandhi College to Kathmandu (Fig. 4); in post-monsoon also a similar pattern is observed. The pre-monsoon AODs are more or less comparable across the IGP and the Himalayas, while during monsoon AOD decreases from Gandhi College to Kathmandu due to precipitation and associated removal of aerosols (as discussed earlier). AODs are quite low over high-altitude locations (e.g., Jomsom, Mt. Everest and Nam Co) in the Himalayas, however, seasonal features are similar to that of Pokhara and Kathmandu (pre-monsoon high and winter low). FMF is the lowest (< 0.75) for Karachi during the year, and is lower than 0.5 during pre-monsoon and monsoon (Fig. 4b). FMF is lower during pre-monsoon and monsoon across the IGP due to the increase in the abundance of dust and sea salt in coarse mode, whereas over the Himalayas it is due to the presence of coarse mode dust/soil particles from the dry and barren lands surrounding Pokhara Valley. Sea salt particles are not significant over the Himalayas (Tripathee et al., 2017). The α values corroborate the features observed in FMF (Fig. 4c) consistent with the type and size of

aerosols that dominate IGP and the Himalayas during different seasons. This comparison illustrates that though FMF (indicating the dominant aerosol size) and α (capturing the spectral distribution of AODs) are comparable the column content (AOD) features differ because of differences in aerosol emission sources and transport of various types of aerosol species to individual sites.

3.2. Fire count and its influence on aerosol properties

The annual mean AOD (meanof 2010–2017) is quite high during the year over the IGP and the surrounding regions (Fig. 5a). Further, on a regional scale during the 8-year period (2010–2017) the AODs are highest during the 2016 pre-monsoon (Fig. 5b), particularly in the month of April (Fig. 5c). The 2016 pre-monsoon seasonal mean AOD is 0.97 ± 0.38 (Fig. 3), and the monthly mean AOD for the 2016 April is 1.37 ± 0.69. The emissions from forest fires and biomass burning including agricultural waste burning contributes significantly to AODs over the Pokhara Valley and the surrounding regions (e.g., Singh et al., 2019). However, the sources of fires vary seasonally - agro-residue burning and forest fires are prevalent during pre-monsoon season, while crop waste burning also occurs during post-monsoon season; in addition emissions from biomass used in domestic cooking is active throughout the year (Lüthi et al., 2015; Bhardwaj et al., 2018; Mahata et al., 2018; Singh et al., 2019). The fires occur throughout the year over the Pokhara Valley and the surrounding regions (Table 1), however, the frequency of fire counts exhibit temporal and spatial variations.

The MODIS fire counts over Pokhara and the surrounding regions peak in April (Table 1, Fig. 6), with 2016 value being the highest among 8 years. The fire counts increase by almost an order of magnitude as the area of coverage surrounding the Pokhara Valley increases (Figs. 5, 6, Table 1). The air mass back trajectories over Pokhara during the year indicate that the origins and trajectories of air parcels vary, and therefore, different aerosol sources from the surrounding regions contribute to the aerosol loading with different characteristics over
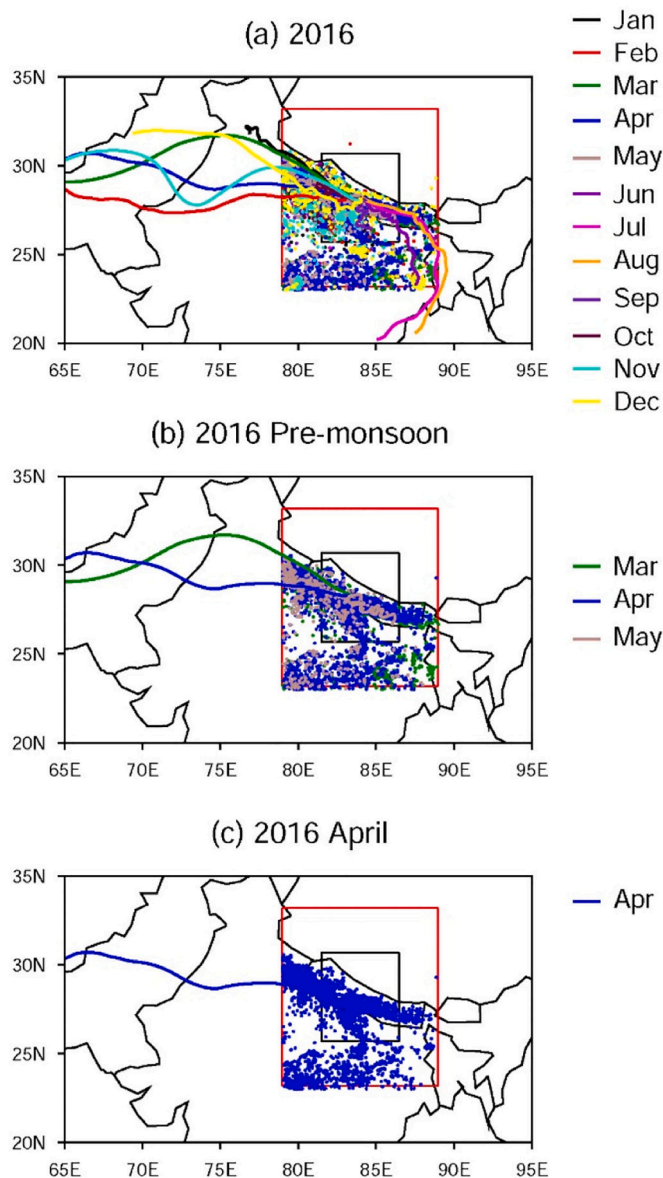
Fig. 6. The MODIS fire counts with confidence value C > 30% assigned the confidence class of nominal and high over Pokhara and the surrounding 5° latitude x 5° longitude, and 10° latitude x 10° longitude regions with Pokhara at the center during (a) 2016 (from January to December), (b) 2016 pre-monsoon (fire counts for the months of March–April-May), and (c) 2016 April. 7-day air mass back trajectories at 500 m above ground level over Pokhara (a) from January to December, (b) for the pre-monsoon months and (c) for April 2016 are also drawn. Note the color of symbols (fire counts) and the lines (representing air mass back trajectories) for each month are the same.

Pokhara (Fig. 6). The fire counts are insignificant during monsoon months (because of precipitation, and wet/moist conditions). The occurrence of fires during March–April (agro-residue burning and forest fires) and November–December (crop waste burning) over north India and the Himalayan foothills give rise to higher fire counts over Pokhara Valley and its surrounding regions (Fig. 6), which is confirmed by the back trajectories as the air masses reaching Pokhara originate and pass over the regions with forest fires and agricultural field-fires (Fig. 6). The fires occur every year during these months, however, the magnitude of the fires show inter-annual variations (Table 1). The AODs follow a similar seasonal cycle as that of fire counts (Figs. 5, 6, Table 1). The fires during March–April contribute the maximum to the total fire counts during the year, however, they exhibit inter-annual variations;

the fires during March–April are minimum during 2015 (30%), and are ≥70% during 2010 and 2016 respectively (Fig. 6, Table 1). The correlation between the monthly mean AOD (calculated from daily means) and total fire counts for the respective months is stronger and significant in April than other months over Pokhara Valley and the surrounding regions (Fig. 7b (correlation coefficient $r = 0.91$, $p = 0.0008$), 7f ($r = 0.97$, $p = 0.004$), and 7j ($r = 0.86$, $p = 0.07$). AODs, and fire counts (over Pokhara and the surrounding regions, Table 1) are lowest in April 2015 (0.36 ± 0.12) and highest in April 2016 respectively (Figs. 3, 5) emphasizing the significant influence the emissions from fires has on aerosol characteristics measured over Pokhara. The correlation is maximum when the difference between the fire counts in the Pokhara Valley and the 5° latitude x 5° longitude grid surrounding the Pokhara is drawn against AOD measured at Pokhara. This result indicates that the fires that occur locally and in the nearby regions (a 5° x 5° region with Pokhara at the center) strongly contribute to the variations in aerosol properties than the fires that occur faraway outside the surrounding 5° x 5° region; this happens despite the fact that the winds pass over both the larger and smaller domains before reaching Pokhara (Fig. 2, 5).

The AODs obtained in April 2016 are the highest over Pokhara which correlates with the concurrent largest number of fires occurred in and around the Pokhara Valley (Table 1, Fig. 7) during the same month. The correlation coefficients are similar when AODs are compared with fire counts obtained over the Pokhara Valley, 5° x 5° region around Pokhara, and 10° x 10° region around Pokhara instead of correlating with differences in fire counts between the respective domains (Figs. 6, 7). This analysis of relation between AOD and fire counts reveals that the influence of local and regional fires on aerosol properties will be more pronounced as compared to distant emissions, and the influence of fires on aerosol properties are distinctly observed every year, heavily contributing to aerosol loading over the Himalayan foothills region, and likely over the Himalayan-Tibetan mountain regions (Lüthi et al., 2015; Singh et al., 2019). These features and correlation between fire counts and AOD can serve as inputs for simulation and prediction of aerosol characteristics over the greater Himalayan regions.

3.3. Size distribution, volume concentration, and effective radius

The seasonal mean aerosol volume size distributions over Pokhara in the 0.05–15 μm radius range are bimodal – with the first peak (at ca. 0.15–0.30 μm) in the fine mode (0.05–1.0 μm) and the second peak (at ca. 4 μm) in the coarse mode (1.0–10.0 μm) (Fig. 8). The aerosol volume size distributions show distinct seasonal variations. The fine mode volume concentration is higher than coarse mode during post-monsoon and winter. The coarse mode volume concentration is comparable to or higher than fine mode volume concentration during pre-monsoon and monsoon. The volume concentration is higher during pre-monsoon as compared to other seasons (Fig. 8). Post monsoon the volume concentrations start increasing more significantly in the fine mode range than in the coarse mode size range (Fig. 8) as coarse mode particles are more efficiently removed due to wet deposition. The peaks in both fine mode and the coarse mode occur at a smaller radius during monsoon as compared to other seasons in the year, indicating the influence of local combustion sources during these months as the regional emissions and transport are suppressed by rain. The volume aerosol size distributions and concentrations in fine mode during 2015 monsoon and post-monsoon are the highest (Figs. 8, 9); the size distribution in fine mode is broader in 2015 post-monsoon than other years (Fig. 8). The volume concentrations in coarse mode are ca. 1.5–2 times higher than fine mode volume concentrations (Fig. 9). The seasonal average volume size distribution obtained in 2016 pre-monsoon is the highest among all the other seasons and years over Pokhara (Figs. 8, 9). The fires peaked during April 2016 on local and regional scales (Table 1), and in April 2010 at a local scale (Table 1), which clearly showed that these record fires heavily influenced the aerosol loadings and their characteristics in
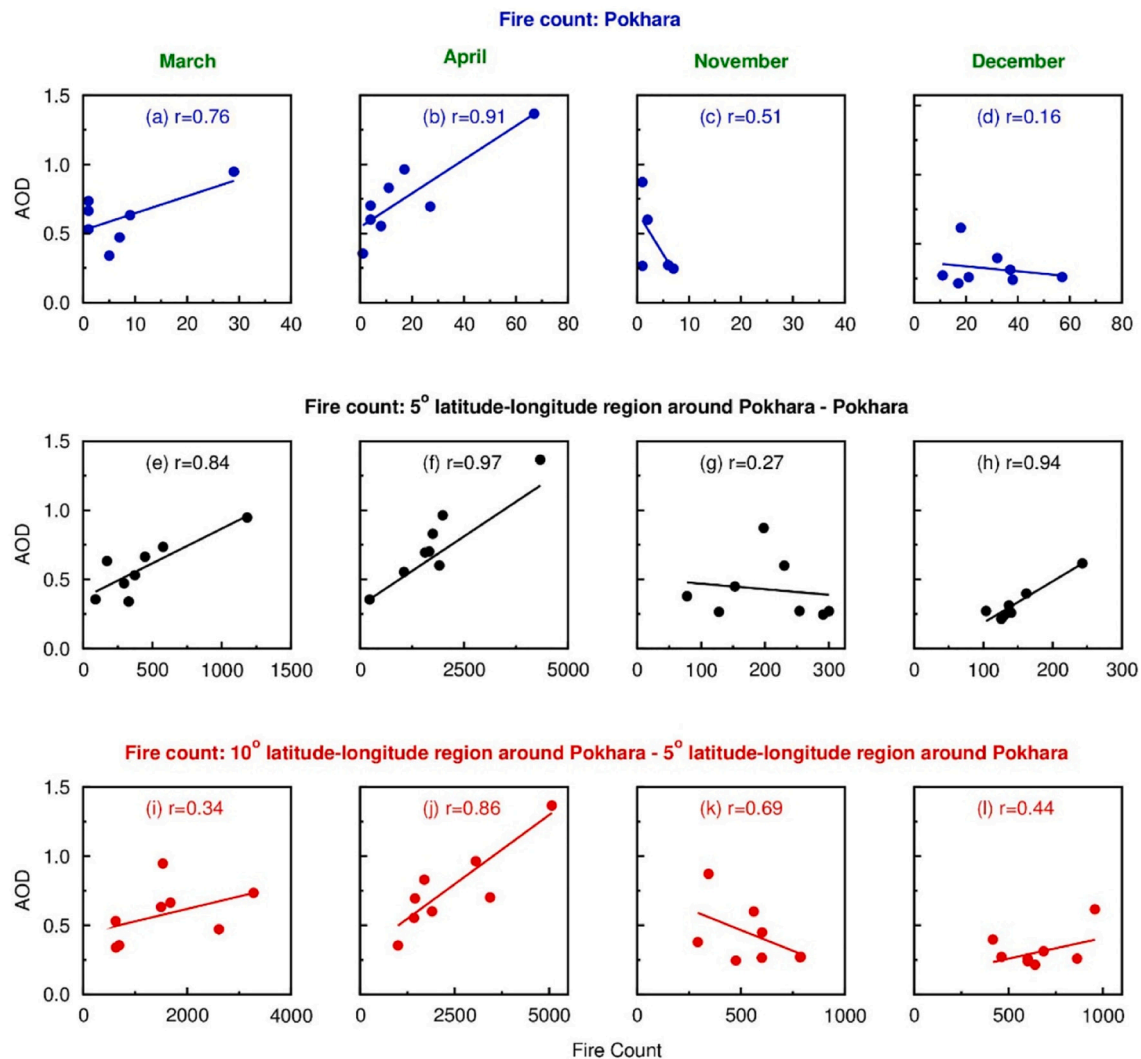
Fig. 7. Correlation between AOD at Pokhara and fire counts in and around the Pokhara Valley during (a) March, (b) April, (c) November and (d) December. Correlation between AOD at Pokhara with fire counts obtained in 5° latitude x 5° longitude region around Pokhara minus the fire counts obtained in the Pokhara Valley (black boxed area in Fig. 5) (a-d) for (e) March, (f) April, (g) November and (h) December. Same as above except that the fire counts now correspond to the difference between those obtained in the 10° x 10° (red boxed area in Fig. 5) and 5° x 5° region (black boxed area in Fig. 5) around Pokhara for (i) March, (j) April, (k) November and (l) December. See text for details.

the region.

The highest increase in fine mode aerosol concentration in 2016 pre-monsoon can clearly be attributed to the emissions from biomass burning (fires) which is quite high on local and regional scales. In contrast in 2010 pre-monsoon the increase in volume size distribution is seen only in coarse mode. The increase in aerosol volume in fine mode is a signature of biomass burning emissions, while the increase in coarse mode volume could be due to either aging and condensation of organic material emitted from fires (Pósfai et al., 2003), and/or due to transport of dust particles (which are larger in size). In all the 8 years, the volume size distributions during pre-monsoon months are marked by an increase in coarse mode aerosol volume. The effects of inter-annual meteorological variations are expected to be relatively small (~5%) on aerosol variations (Zhang et al., 2019), here the volume concentrations in the coarse mode have increased almost by an order of magnitude (Fig. 9b). The significant increase in the volume of larger size aerosols (> 1 μm) during 2016 pre-monsoon (Fig. 9b) emphasizes the influence of emissions from fires on coarse mode aerosols as well. As the influence of inter-annual meteorological variations were negligible, and the increase in higher size aerosol volume is due to transport of dust or soil particles during pre-monsoon (seen every year), the increase in coarse

mode volume over and above due to dust can be quantified to be due to the huge increase in fires during April 2010 and 2016 in and around Pokhara. In addition, the relative difference in fire counts during April 2010 and April 2016 (Table 1) can be seen contributing to differences in coarse mode aerosol volume, in addition to, the changes in composition and aging of aerosols. These findings are corroborated by the higher volume concentration in fine, coarse modes and their total in 2010 and 2016 pre-monsoon respectively (Fig. 9). The aerosol volume size distributions, and volume concentrations in 2015 monsoon in fine and coarse mode increase significantly; the fine mode concentration in 2015 monsoon is the highest during monsoon among all the 8-years (Figs. 8, 9) leading to a large increase in AOD (Fig. 3), this is similar in 2010 monsoon also. The fine mode concentration peaks at a higher radius in fine mode during 2011 post-monsoon (Fig. 8) resulting in the highest effective radius (Fig. 10), and AOD during post-monsoon (Fig. 3). The observance of such intricate features in seasonal and inter-annual variations in aerosol characteristics is possible only due to the synergistic analysis of both optical and physical properties in fine and coarse size ranges.

The effective radius (r_e), i.e., surface area-weighted mean radius of aerosols, a measure of the total volume to the surface area of an aerosol
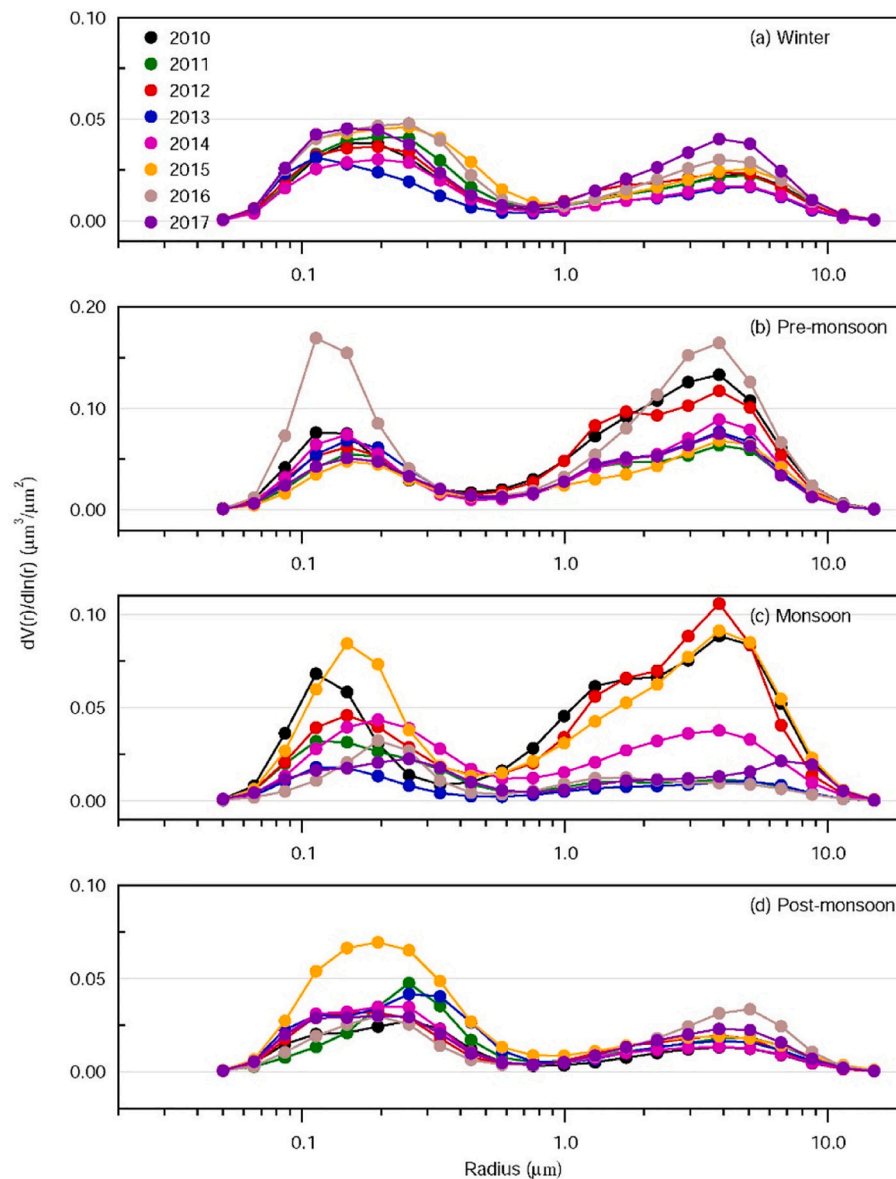
Fig. 8. Seasonal average aerosol volume size distributions in the 0.05 to 15 μm radius range over Pokhara for (a) winter, (b) pre-monsoon, (c) monsoon and (d) post-monsoon during an 8-year (2010–17) period of measurement. Note y-axis scale in (b) is twice that of (a), (c) and (d).

size distribution, of the coarse mode aerosols is an order of magnitude higher than the fine mode aerosols during the year (Fig. 10). The r_e of fine mode aerosols remains more or less same (> 0.1 and < 0.2 μm) during the year over Pokhara, whereas the r_e of coarse mode aerosols decreases gradually from winter to monsoon. However, owing to the large increase in the coarse mode volume concentration (lowering the α value significantly) the r_e of total aerosol increases significantly during monsoon compared to the other seasons. The variations observed in AOD, FMF and α (Fig. 3) are consistent with the seasonal change in aerosol size distribution over Pokhara. In the 8-year period, r_e is highest for coarse and higher for fine mode aerosols in 2017 monsoon, however, the volume concentrations in fine and coarse mode size ranges are comparable (Fig. 9), confirming an increase in the aerosol concentration in both size ranges as revealed by the aerosol size distribution (Fig. 8). The r_e of 2010, 2012 and 2015 monsoon and volume concentrations in coarse mode are comparable consistent with the aerosol size distributions (Fig. 8). The volume aerosol size distributions in the coarse mode is significantly higher in these three years (Fig. 8). A higher FMF occurs due to the dominance of fine mode aerosols in the size distribution while a lower FMF arises due to the abundance of

coarse mode aerosols (Fig. 3). The FMF is > 0.8 during post-monsoon, and winter (Fig. 3). During these seasons the fine mode size distribution, and volume concentration are higher or almost equal to the coarse mode; however, during pre-monsoon and monsoon the coarse mode volume concentrations are greater than fine mode volume concentrations. These results on volume size distributions compare well with those obtained over three locations (Ilorin, Nigeria; Kanpur, India; Beijing, China) with aerosol mixtures composed of coarse dust combined with fine mode combustion generated aerosols from fossil fuel and biomass burning sources (Eck et al., 2010). The features of columnar aerosol size distribution, volume concentration and effective radii obtained over Pokhara exhibit characteristics as that of urban/industrial, biomass burning and dust influenced location(s). Over the locations affected by urban/industrial mixed and biomass burning emissions the fine mode volume is higher than that of coarse mode volume (Dubovik et al., 2002) as seen during post-monsoon and winter months in Pokhara; the coarse mode volume is higher than fine mode when the location is influenced by dust as in pre-monsoon over Pokhara. The coarse mode r_e for a dust influenced location (r_e = 2.3–2.5 μm) is significantly lower than that of urban/industrial
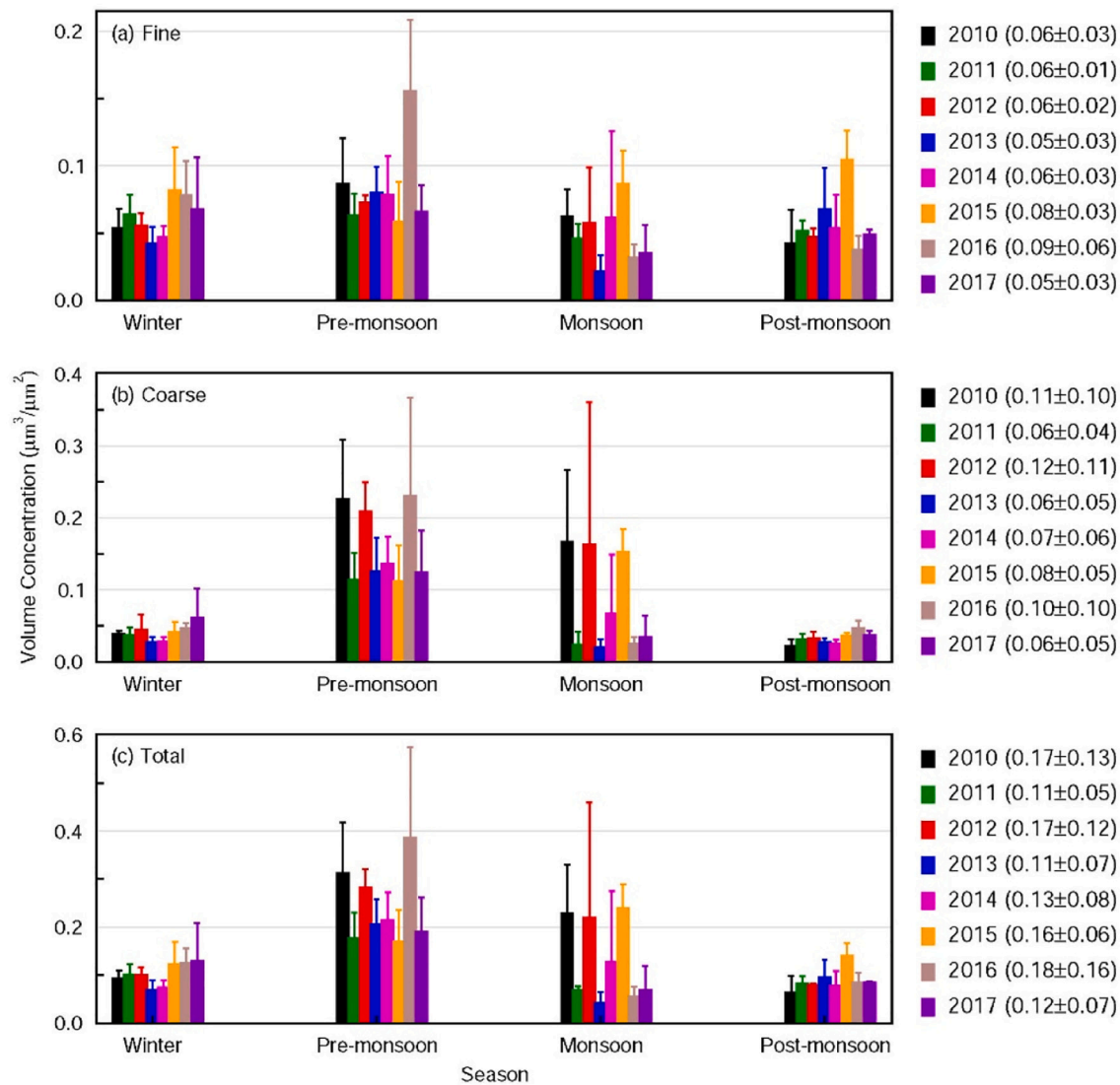
Fig. 9. Seasonal mean aerosol volume concentration during 2010–17 over Pokhara in the (a) fine, (b) coarse modes, and (c) their total. The numbers on the right hand side of each panel show the annual mean with a standard deviation from the mean for each year.

and biomass burning aerosols (r_e = 3.0–3.3 μm), while the fine mode r_e in all the above types of locations lie in an almost similar (r_e = 0.11–0.15 μm) radius range (Dubovik et al., 2002). The coarse mode r_e decreases (to 2 μm or less) in Pokhara when the abundance of coarse mode dust particles increases in size distribution (Fig. 10) in pre-monsoon while the fine mode r_e remains more or less in the same range throughout the year (0.1–0.2 μm). The very similar features in aerosol size distribution, volume concentration and effective radius every year over Pokhara (influenced by an urban/industrial, biomass burning and dust sources at different times in the year) can significantly help in improving the characterization/parameterization of aerosol properties over high-altitude locations in the Himalayas.

4. Conclusions

This study provides a summary of a comprehensive analysis of the seasonal and inter-annual variations of all key optical and physical properties of columnar aerosols performed for the first time over the Pokhara Valley, a site in the Himalayan foothills located in close premises of heavily polluted Indo-Gangetic Plain (IGP) to the south and the relatively cleaner Himalayan mountains to the north from the high-quality ground-based columnar aerosol data obtained recently for a

period of eight years from January 2010 to December 2017, including the influence of emissions from forest fires and agricultural field fires on aerosol properties. The AODs and other aerosol properties show remarkable and consistent seasonal cycle every year. The seasonal mean AODs over Pokhara are higher during eight months of the year from October to May (winter, pre-monsoon and post-monsoon months) – high enough to classify as a polluted site, and lower during four months (in monsoon season). The peak AOD during pre-monsoon is attributed to the stronger convective activity in the IGP and the Himalayan foothills due to which polluted air masses are mixed with westerlies and move eastwards/northwards to the mountain regions, and also stronger local mountain-valley circulations in the complex mountainous region, and give rise to higher AOD every year. The FMF and α (which defines the spectral distribution of AODs) corroborate the seasonal pattern of AODs. A comparison of aerosol optical properties reveals that though α values are comparable between Kanpur (an urban location influenced by dust in the IGP), Lumbini (a semi-urban location), in the northern edge of the central IGP and Pokhara during the year, the column content (AOD) features differ owing to differences in aerosol emission sources and transport. Emissions from biomass burning (agricultural waste burning) over north India and local emissions in Pokhara (as revealed by the MODIS fire counts) exhibit a good correlation with
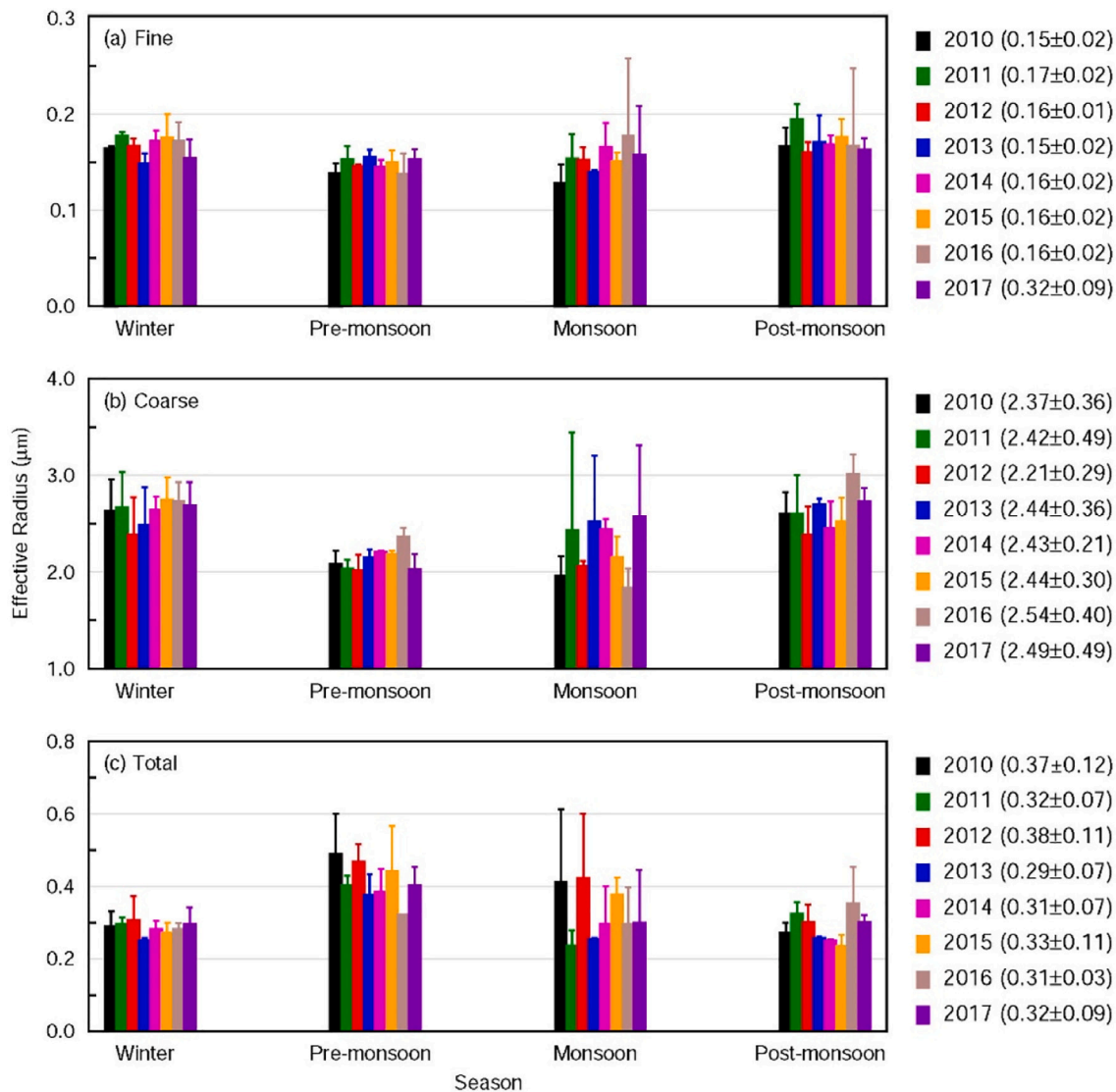
Fig. 10. Seasonal mean effective radius (r_e) of aerosols over Pokhara in various size ranges. (a) fine, (b) coarse, and (c) their total. The numbers on the right hand side of each panel show the annual mean with a standard deviation from the mean for each year.

AODs measured over Pokhara. The correlation between AOD and fire counts over (i) the vicinity of the measurement location and (ii) the nearby surrounding the Pokhara Valley is maximum suggesting that the fires in these two regions strongly contribute to the variations in aerosol properties over the Himalayan foothills region than the fires that occur faraway.

The columnar volume aerosol size distributions are bimodal – with the first peak in the fine mode (0.05–1.0 μm) and the second peak in the coarse mode (1.0–10.0 μm), and exhibit distinct seasonal variations. The fine mode volume concentration is higher than coarse mode during post-monsoon and winter, whereas the coarse mode volume concentration is either comparable to or higher than fine mode volume concentration during pre-monsoon and monsoon. The volume size distribution obtained in 2016 pre-monsoon is the highest among all the years and seasons during which the fire counts were also highest during 2010–2017 on local and regional scales. The effective radius (r_e) of the coarse mode aerosols is an order of magnitude higher than the fine mode aerosols throughout the year. The fine mode r_e remains more or less same (between 0.1 and 0.2 μm) during the year, whereas the r_e of coarse mode aerosols decreases gradually from winter to monsoon. However, owing to the large increase in the coarse mode volume concentration (lowering the α value significantly) the r_e of total aerosol

increases significantly during monsoon when compared to the other seasons. Results obtained on volume size distributions over Pokhara compare well with those obtained over three locations (Ilorin, Nigeria; Kanpur, India; and Beijing, China) which are dominated by aerosol mixtures composed of coarse dust combined with fine mode combustion generated aerosols from fossil fuel and biomass burning sources. Such a detailed analysis on the similar seasonal features in AOD, FMF, spectral variation (α), volume size distribution, volume concentration and effective radius every year over Pokhara, which are resulted from the influence of urban/industrial, biomass burning and dust sources at different times in the year, and their correlation with fire counts can significantly help in improving the characterization/parameterization of aerosol properties and quantification of their impacts on air quality, climate and sensitive ecosystems over the high-altitude locations in the Himalayas and the surrounding mountain regions, which are still a relatively poorly sampled and studied regions of the world.

Author contributions

SR designed the study in consultation with MR. SR performed the analysis and wrote the paper. Both the authors reviewed and edited the paper.

Data availability

All data used in the manuscript are publicly available at http://www.esrl.noaa.gov/psd/, https://giovanni.gsfc.nasa.gov/giovanni/, https://firms.modaps.eosdis.nasa.gov/ and https://aeronet.gsfc.nasa.gov/, ram@prl.res.in, srikanthan.ramachandran@iass-potsdam.de, maheswar.rupakheti@iass-potsdam.de

Declaration of Competing Interest

The authors declare no competing financial interests.

Acknowledgments

References

Bhardwaj, P., Naja, M., Rupakheti, M., Lupascu, A., Mues, A., Panday, A.K., Kumar, R., Mahata, K.S., Lal, S., Chandola, H.C., Lawrence, M.G., 2018. Variations in ozone and carbon monoxide in the Kathmandu Valley and surrounding broader regions during SusKat-ABC field campaign: role of local and regional sources. Atmos. Chem. Phys. 18, 11949–11971.

Chen, P.F., Kang, S., Li, C., Zhang, Q., Guo, J., Tripathee, L., Zhang, Y., Li, G., Gul, C., Cong, Z., Wan, X., Niu, H., Panday, A.K., Rupakheti, M., Ji, Z., 2019. Carbonaceous aerosol characteristics on the Third Pole: a primary study based on the atmospheric pollution and cryospheric change (APCC) network. Environ. Pollut. 253, 49–60.

Cho, C., Kim, S.-W., Rupakheti, M., Park, J.-S., Panday, A., Yoon, S.-C., Kim, J.-H., Kim, H., Jeon, H., Sung, M., Kim, B.M., Hong, S.K., Park, R.J., Rupakheti, D., Mahata, K.S., Praveen, P.S., Lawrence, M.G., Holben, B., 2017. Wintertime aerosol optical and radiative properties in the Kathmandu Valley during the SusKat-ABC field campaign. Atmos. Chem. Phys. 17, 12617–12632.

Dubovik, O., Smirnov, A., Holben, B.N., King, M.D., Kaufman, Y.J., Eck, T.F., Schuster, I., 2000. Accuracy assessments of aerosol optical properties retrieved from Aerosol Robotic Network (AERONET) Sun and Sky radiance measurements. J. Geophys. Res. 105, 9791–9806.

Dubovik, O., Holben, B., Eck, T.F., Smirnov, A., Kaufman, Y.J., King, M.D., Tanre, D., Slutsker, I., 2002. Variability of absorption and optical properties of key aerosol types observed in worldwide locations. J. Atmos. Sci. 59, 590–608.

Eck, T.F., Holben, B.N., Sinyuk, A., Pinker, R.T., Goloub, P., Chen, H., Chatenet, B., Li, Z., Singh, R.P., Tripathi, S.N., Reid, J.S., Giles, D.M., Dubovik, O., O'Neill, N.T., Smirnov, A., Wang, P., Xia, X., 2010. Climatological aspects of the optical properties of fine/coarse mode aerosol mixtures. J. Geophys. Res. 115, D19205. https://doi.org/10.1029/2010JD014002.

García, O.E., Diaz, A.M., Expósito, F.J., Diaz, J.P., Dubovik, O., Dubuisson, P., Roger, J.-C., Eck, T.F., Sinyuk, A., Derimian, Y., Dutton, E.G., Schafer, J.S., Holben, B.N., García, A., 2008. Validation of AERONET estimates of atmospheric solar fluxes and aerosol radiative forcing by ground-based broadband measurements. J. Geophys. Res. 113. https://doi.org/10.1029/2008JD010211.

Gautam, R., Hsu, N.C., Tsay, S.C., Lau, K.M., Holben, B., Bell, S., Smirnov, A., Li, C.,

Hansell, R., Ji, Q., Payra, S., Aryal, D., Kayastha, R., Kim, K.M., 2011. Accumulation of aerosols over the Indo-Gangetic plains and southern slopes of the Himalayas: distribution, properties and radiative effects during the 2009 pre-monsoon season. Atmos. Chem. Phys. 11, 12841–12863.

Giglio, L., Schroeder, W., Justice, C.O., 2016. The collection 6 MODIS active fire detection algorithm and fire products. Remote Sens. Environ. 78, 31–41.

Gustafsson, O., Ramanathan, V., 2016. Convergence on climate warming by black carbon aerosols. PNAS 113, 4243–4245.

Holben, B.N., Tanré, D., Smirov, A., Eck, T.F., Slutsker, I., Abuhassan, N., Newcomb, W.W., Schafer, J.S., Chatenet, B., Lavenu, F., Kaufman, Y.J., Vande Castle, J., Setzer, A., Markham, B., Clark, D., Frouin, R., Halthore, R., Karneli, A., O'Neill, N.T., Pietras, C., Pinker, R.T., Voss, K., Zibordi, G., 2001. An emerging ground-based aerosol climatology: aerosol optical depth from AERONET. J. Geophys. Res. 106, 12067–12097.

IPCC, 2013. Summary for Policymakers in Climate Change 2013: The Physical Science Basis. In: Stocker, T.F., Qin, D., Plattner, G.-K., Tignor, M., Allen, S.K., Boschung, J. ... Midgley, P.M (Eds.), Contribution of Working Group I to the Fifth Assessment Report of the Intergovernmental Panel on Climate Change. Cambridge University Press, Cambridge, UK and New York, NY, USA, pp. 1–33.

Kedia, S., Ramachandran, S., Tripathi, S.N., Holben, B., 2014. Quantification of aerosol type, and sources of aerosols over the Indo-Gangetic Plain. Atmos. Environ. 98, 607–619.

Kuhlmann, J., Quaas, J., 2010. How can aerosols affect the Asian summer monsoon? Assessment during three consecutive pre-monsoon seasons from CALIPSO satellite data. Atmos. Chem. Phys. 10, 4673–4688.

Lawrence, M.G., Lelieveld, J., 2010. Atmospheric pollutant outflow from southern Asia: a review. Atmos. Chem. Phys. 10, 11017–11096.

Levy, R.C., Mattoo, S., Munchak, L.A., Remer, L.A., Sayer, A.M., Patadia, F., Hsu, N.C., 2013. The collection 6 MODIS aerosol products over land and ocean. Atmos. Meas. Tech. 6, 2989–3034.

Lüthi, Z.L., Skerlak, B., Kim, S.W., Lauer, A., Mues, A., Rupakheti, M., Kang, S.C., 2015. Atmospheric brown clouds reach the Tibetan Plateau by crossing the Himalayas. Atmos. Chem. Phys. 15, 6007–6021.

Mahata, K.S., Rupakheti, M., Panday, A.K., Bhardwaj, P., Naja, M., Singh, A., Mues, A., Cristofanelli, P., Pudasainee, D., Bonasoni, P., Lawrence, M.G., 2018. Observation and analysis of spatiotemporal characteristics of surface ozone and carbon monoxide in the Kathmandu Valley, Nepal. Atmos. Chem. Phys. 18, 14113–14132.

Meng, J., Yang, H., Yi, K., Liu, J., Guan, D., Liu, Z., Mi, Z., Coffman, D'.M., Wang, X., Zhong, Q., Huang, T., Meng, W., Tao, S., 2019. The slowdown in global air-pollutant emission growth and driving factors. One Earth 1, 136–148.

Myhre, G., Samset, B.H., Schulz, M., Balkanski, Y., Bauer, S., Berntsen, T.K., Bian, H., Bellouin, N., Chin, M., Diehl, T., Easter, R.C., Feichter, J., Ghan, S.J., Hauglustaine, D., Iversen, T., Kinne, S., Kirkevåg, A., Lamarque, J.-F., Lin, G., Liu, X., Lund, M.T., Luo, G., Ma, X., van Noije, T., Penner, J.E., Rasch, P.J., Ruiz, A., Seland, Ø., Skeie, R.B., Stier, P., Takemura, T., Tsigaridis, K., Wang, P., Wang, Z., Xu, L., Yu, H., Yu, F., Yoon, J.-H., Zhang, K., Zhang, H., Zhou, C., 2013. Radiative forcing of the direct aerosol effect from AeroCom phase II simulations. Atmos. Chem. Phys. 13, 1853–1877.

O'Neill, N.T., Eck, T.F., Smirnov, A., Holben, B.N., Thulasiraman, S., 2003. Spectral discrimination of coarse and fine mode optical depth. J. Geophys. Res. 108 (doi). https://doi.org/10.1029/2002JD002975.

Pósfai, M., Simonics, R., Li, J., Hobbs, P.V., Buseck, P.R., 2003. Individual aerosol particles from biomass burning in southern Africa, 1, Compositions and size distributions of carbonaceous particles. J. Geophys. Res. 108, 8483. https://doi.org/10.1029/2002JD002291.

Putero, D., Marinoni, A., Bonasoni, P., Calzolari, F., Rupakheti, M., Cristofanelli, P., 2018. Black carbon and ozone variability at the Kathmandu Valley and at the southern Himalayas: a comparison between a "hot spot" and a downwind high-altitude site. Aerosol Air Qual. Res. 18, 623–635.

Raatikainen, T., Hyvärinen, A.-P., Hatakka, J., Panwar, T.S., Hooda, R.K., Sharma, V.P., Lihavainen, H., 2014. The effect of boundary layer dynamics on aerosol properties at the Indo-Gangetic plains and at the foothills of the Himalayas. Atmos. Environ. 89, 548–555.

Ramanathan, V., Li, F., Ramana, M.V., Praveen, P.S., Kim, D., Corrigan, C.E., Nguyen, H., Stone, E.A., Schauer, J.J., Carmichael, G.R., Adhikary, B., Yoon, S.C., 2007a. Atmospheric brown clouds: Hemispherical and regional variations in long-range transport, absorption, and radiative forcing. J. Geophys. Res. 112. https://doi.org/10.1029/2006JD008124.

Ramanathan, V., Ramana, M.V., Roberts, M., Kim, D., Corrigan, C., Chung, C., Winker, D., 2007b. Warming trends in Asia amplified by brown cloud absorption. Nature 448, 575–579.

Rupakheti, D., Adhikary, B., Praveen, P.S., Rupakheti, M., Kang, S., Mahata, K.S., Naja, M., Zhang, Q., Panday, A.K., Lawrence, M.G., 2017. Pre-monsoon air quality over Lumbini, a world heritage site along the Himalayan foothills. Atmos. Chem. Phys. 17 (11041–11063), 2017.

Rupakheti, D., Kang, S., Rupakheti, M., Cong, Z., Tripathee, L., Panday, A.K., Holben, B.N., 2018. Observation of optical properties and sources of aerosols at Buddha's birthplace, Lumbini, Nepal: environmental implications. Environ. Sci. Pollut. Res. 25, 14868–14881.

Rupakheti, D., Kang, S., Rupakheti, M., Cong, Z., Panday, A.K., Holben, B.N., 2019. Identification of absorbing aerosol types at a site in the northern edge of Indo-Gangetic Plain and a polluted valley in the foothills of the central Himalaya. Atmos. Res. 223, 15–23.

Rupakheti, D., Kang, S., Rupakheti, M., 2020. Two heavy haze events over Lumbini in South Nepal: Enhanced aerosol radiative forcing and heating rates. Atmos. Environ. 236, 117658. https://doi.org/10.1016/j.atmosenv.2020.117658.

Saikawa, E., Panday, A., Kang, S., Gautam, R., Zusman, E., Cong, Z., Somanathan, E.,

Adikary, B., Yokelson, R.E., Crawford, J.H., Rupakheti, M., Ye, W.L., Saroar, M.G., 2019. In: Wester, P., Mishra, A., Mukherji, A., Shrestha, A.B. (Eds.), Air Pollution in the Hindu Kush Himalaya in *The Hindu Kush Himalaya Assessment*. Springer, pp. 339–377.

Singh, A., Mahata, K.S., Rupakheti, M., Junkermann, W., Panday, A.K., Lawrence, M.G., 2019. An overview of airborne measurement in Nepal – part 1: Vertical profile of aerosol size, number, spectral absorption, and meteorology. Atmos. Chem. Phys. 19, 245–258.

Tripathee, L., Kang, S., Rupakheti, D., Cong, Z., Zhang, Q., Huang, J., 2017. Chemical characteristics of soluble aerosols over the Central Himalayas: insight into spatio-temporal variations and sources. Environ. Sci. Pollut. Res. 24, 24454–24472.

Zhang, Q., Zheng, Y., Tong, D., Shao, M., Wang, S., Zhang, Y., Xu, X., Wang, J., He, H., Liu, W., Ding, Y., Lei, Y., Li, J., Wang, Z., Zhang, X., Wang, Y., Cheng, J., Liu, Y., Shi, Q., Yan, L., Geng, G., Hong, C., Li, M., Liu, F., Zheng, B., Cao, J., Ding, A., Gao, J., Fu, Q., Hua, J., Liu, B., Liu, Z., Yang, F., He, K., Hao, J., 2019. Drivers of improved $PM_{2.5}$ air quality in China from 2013 to 2017. PNAS. https://doi.org/10.1073/pnas.1907956116.